

# Interferometric precision measurements with Bose–Einstein condensate solitons formed by an optical lattice

N. Veretenov, Yu. Rozhdestvensky<sup>a</sup>, N. Rosanov, V. Smirnov, and S. Fedorov

S.I. Vavilov State Optical Institute, Research Institute for Laser Physics, Birzhevaya Line 12, 199034 St. Petersburg, Russia

Received 15 November 2005 / Received in final form 7 July 2006

Published online 23 March 2007 – © EDP Sciences, Società Italiana di Fisica, Springer-Verlag 2007

**Abstract.** We propose the precision measurement of both angular rotation and of the gradient magnetic of a field based on the use of matter wave interferometers with soliton states of a Bose-Einstein condensate (BEC). We consider the formation of these soliton states in a BEC with negative scattering length by an optical lattice produced by two counterpropagating laser beams. We determine the parameters of both the initial condensate and the optical radiation necessary for the formation of coherent solitons. We demonstrate that this interferometer can be used to measure magnetic field gradient with a precision of  $10^{-2}$  pT/cm. Our calculations show that the sensitivity of a gyroscope based on a ring, two-port matter wave interferometer can achieve  $2.6 \times 10^{-7}$  rad s<sup>-1</sup>. The precision of this method is more than ten times greater than in that of rotating interferometer with cooled atoms.

**PACS.** 03.75.Dg Atom and neutron interferometry – 42.50.Vk Mechanical effects of light on atoms – 07.60.Ly Interferometers – 42.87.Bg Phase shifting interferometry

## 1 Introduction

As atomic Bose-Einstein condensates (BEC) are in wide use in a large number of laboratories, of great importance is the question of possible applications of such a macroscopic quantum object in the fundamental and applied science [1–6]. One of the promising applications of a BEC is in the measurement of different physical quantities with high precision. In fact, a BEC is almost an ideal tool for precision measurement as it is very sensitive to influence from external factors. The key to using a BEC for precision measurements is the coherent construction of its spatial state. This is, for example, the case in the interaction between optical and matter waves where BEC splitting into a number of momentum groups is used [1], and in mode-locked atom lasers [3] where the BEC wave function is spatially modulated by a periodic optical potential, see also [4]. Recent observations of soliton states of Li atoms in a cylindrical optical trap [5] (see also [6]) open up new possibilities in the field of BEC applications such as frequency stabilization [7] and nanolithography based on the formation of ultra-narrow spatial BEC solitons [8].

In this paper we examine possibilities for the use of spatial soliton states in a BEC with negative scattering length for the goal of atomic interferometry. The first step in the scheme considered is the formation of spatial soliton states from a BEC by an optical lattice produced by two counterpropagating laser beams. Next, we demonstrate

that the use of different types of atomic interferometers with two BEC solitons as input beams allows one to make precision measurements of both magnetic field gradient and angular rotation.

## 2 Model

We consider a BEC consisting of  $N$  atoms of mass  $M$  at temperature less than the critical one, placed in an optical lattice formed by two counterpropagating laser beams with wave numbers  $k$ , frequency  $\omega$ , and electric field strength:

$$E(z, t) = E_0[e^{i(kz-\omega t)} + e^{i(kz+\omega t)} + c.c.]. \quad (1)$$

We use the two-level approximation for the atomic system and define the detuning  $\Delta$  from the atomic resonance as  $\Delta = \omega - \omega_0$  where  $\omega_0$  is the atomic transition frequency. In order to avoid the effect of spontaneous emission we use light far from resonance,  $|\Delta| \gg \gamma$ , where  $\gamma$  is the spontaneous decay rate of the excited atomic level. The coupling of the light field from equation (1) to the atomic system is characterized by the Rabi frequency  $\Omega = dE_0/2\hbar$ , where  $d$  is the dipole matrix element of the transition. If the Rabi frequency is much smaller than the detuning  $\Omega \ll |\Delta|$ , we can adiabatically eliminate the excited level of the atomic system [1]. Moreover, the rotating wave approximation can be used, and the terms varying at twice the optical frequency  $\omega$  can be neglected.

<sup>a</sup> e-mail: rozd-yu@mail.ru

We will assume also that the BEC is well confined along the  $z$ -axis, so that the system can be described by a spatially one-dimensional time-dependent Gross-Pitaevskii equation (GPE) for the condensate one-particle wave function  $\Phi(z, t)$  of the atom ground state

$$i\hbar \frac{\partial \Phi}{\partial t} = -\frac{\hbar^2}{2M} \frac{\partial^2 \Phi}{\partial z^2} + V(z)\Phi - \frac{4\pi\hbar^2 a}{M} \frac{N}{\sigma} |\Phi|^2 \Phi. \quad (2)$$

Here  $V(z) = V_0 \cos^2(kz)$  is the optical potential for the atomic ground level,  $V_0 = \hbar\Omega^2/\Delta$  is the lattice depth,  $a$  is the modulus of the scattering length, which is taken to be negative,  $\sigma = 2\pi\hbar/M\omega_c$  is the BEC area transverse to the  $z$ -axis [9], and  $\omega_c$  is the oscillation frequency of the atoms in the waveguide. The condensate wave function  $\Phi(z, t)$  is normalized as follows:

$$\int_{-\infty}^{\infty} |\Phi|^2 dz = 1. \quad (3)$$

After introducing the dimensionless variables  $z' = z/z_c$ ,  $t' = t/t_c$ ,  $t_c = 2Mz_c^2/\hbar$ , the GPE (2) for the function  $\Psi(z', t') = (8\pi a z_c^2 N/\sigma)^{1/2} \Phi(z, t)$  takes the form

$$i \frac{\partial \Psi}{\partial t'} = -\frac{\partial^2 \Psi}{\partial z'^2} + V(z_c, z')\Psi - |\Psi|^2 \Psi, \quad (4)$$

with the dimensionless amplitude  $V_0^c = (2Mz_c^2/\hbar^2)V_0$  of the optical potential  $V(z_c, z') = V_0^c \cos^2(kz_c z')$ . We assume also that the initial wave function of the BEC, which is formed in a magnetic trap, has the Gaussian shape

$$\Psi(z', t = 0) = \exp[-(z'/w)^2], \quad (5)$$

with a width  $w = 15$  much larger than the width of a soliton with maximum amplitude  $\Psi_s = 1$ . The maximum concentration in the initial condensate described by (5) is determined by the spatial scale factor  $z_c$  as

$$N_c^m = \frac{N |\Phi(0, 0)|^2}{\sigma} = \frac{1}{8\pi a z_c^2}. \quad (6)$$

Expressing  $\Phi(z)$  through  $\Psi(z')$  and using (3), we obtain after integration over  $z$  the number of atoms in the initial condensate (5), which is found to be

$$N = \frac{15\sigma}{8\sqrt{2\pi} a z_c}. \quad (7)$$

We have to point out that the condition of using an one-dimensional approach [2]

$$\hbar\omega_c < \frac{4\pi\hbar^2 a N}{M\sigma} |\Phi|^2 \quad (8)$$

limits the maximum of the atom concentration in the BEC to

$$N_c^m < \frac{1}{2a\sigma}. \quad (9)$$

In the case of negative scattering length, condition (9) prevents the collapse of the atomic beam in transversal direction as well as in the case of optical self-focusing [10].

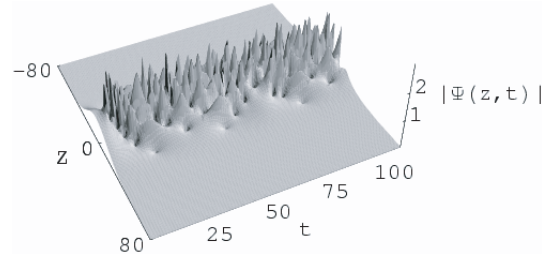


**Fig. 1.** Time evolution of the modulus of the condensate wave function  $|\Psi(z, t)|$  after switching off the magnetic field along the  $z$ -axis. The time scale  $t_c = 1$  ms,  $z_c = 2$   $\mu$ m.

### 3 Formation of BEC solitons by an optical lattice

Let us assume that the initial BEC is located in a magnetic trap. At the moment  $t = t_0$ , the magnetic force along the  $z$ -axis is switched off and the BEC can be considered as free (of course, along the  $z$ -axis only). Such a system is described by a one-dimensional Gross-Pitaevskii equation (2) without the optical potential,  $V(z) = 0$ . Figure 1 demonstrates the time evolution of the modulus of the condensate wave function  $|\Psi(z, t)|$  after switching off the magnetic field. One can see the fast irregular decay of the BEC determined by the modulation instability. An important point is that this decay can be controlled by a light lattice formed by an off-resonant standing optical wave.

Let us examine the conditions of the efficient formation of quasi-soliton structures of a BEC interacting with an optical lattice. We will assume that the optical potential depth  $V_0^c$  is much less than the value of the non-linear term in the right-hand side of equation (4). Then we can carry out the linearization of equation (4), using the optical potential as a small initial perturbation for the condensate wave function [11]. For this purpose we look for the solution of equation (4) for a BEC nearly homogeneous along the  $z$ -axis as

$$\Psi = (1 + \delta\Psi) \exp(it'). \quad (10)$$

Here  $\delta\Psi$  is a small perturbation to the wave function of free the BEC (when the optical potential  $V_0^c = 0$ ). In the general case the perturbation  $\delta\Psi$  can be assumed to take the form

$$\delta\Psi = a_+ \exp(i\chi z' + \alpha t') + a_-^* \exp(-i\chi z' + \alpha^* t'),$$

where  $a_{\pm}$  are constant amplitudes,  $\alpha$  is the perturbation growth rate, and  $\chi = 2kz_c$  is the spatial frequency of periodical perturbations. Substituting this expression in to equation (4) and only keeping terms linear in  $\delta\Psi$ , we obtain

$$\alpha = \chi \sqrt{2 - \chi^2}. \quad (11)$$

Figure 2a displays the dependence of the growth rate of small perturbations on their spatial frequency, as given by numerical simulations of equation (4). As can be seen, the instability area of spatial frequency  $\chi$  is in good agreement with the approximate expression (11). Therefore the condition of exponential increase of small-scale perturbations

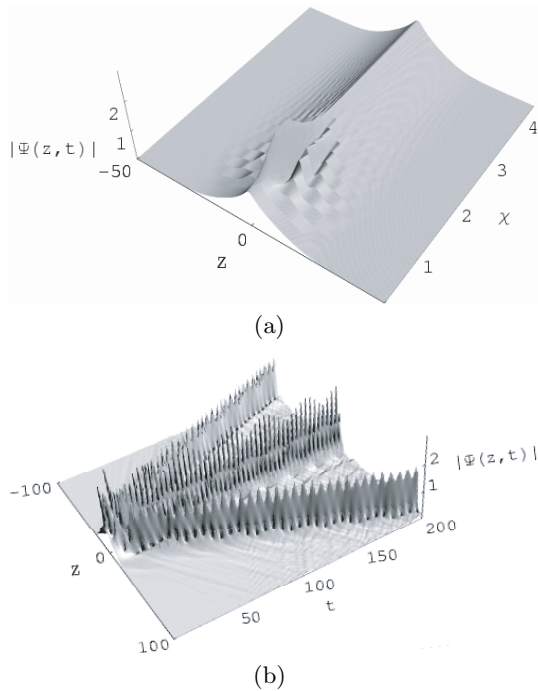


**Fig. 2.** The dependence of magnitude perturbation of the BEC wave function modulus on spatial frequency  $\chi$  for the interaction time  $t = 1.5$  ms (a) and time evolution of the modulus of the condensate wave function  $|\Psi(z, t)|$  after interaction with the optical lattice,  $V_0^c = 0.02$  (b).

is (see also [4])

$$2kz_c \leq \sqrt{2}. \quad (12)$$

Equations (6), (9) show that  $\sigma \leq 4\pi z_c^2$ , i.e. the number of atoms in the initial condensate (5) should satisfy the inequality:

$$N \leq \frac{15}{2} \sqrt{\frac{\pi}{2}} \frac{z_c}{a}. \quad (13)$$

Therefore the scale factor  $z_c$ , which is connected with the laser wave length according to (12), limits the atom number in the condensate. At the same time, the atom concentration in the initial condensate (5) decreases when  $z_c$  increases. Thus the scale factor  $z_c$  determines also the critical temperature  $T_{cr}$  at which a condensate can be formed. Thus, the optimum value of  $z_c$  can be chosen as  $z_c = 2 \mu\text{m}$ . This value  $z_c$  determines the concentration  $N_c^m = 0.7 \times 10^{13} \text{ cm}^{-3}$  and the critical temperature  $T_{cr} \sim (N_c^m)^{1/3} \approx 10^{-7} \text{ K}$  [12] together with the condensate cross-section  $\sigma \leq 5 \times 10^{-7} \text{ cm}^2$ , i.e. the radius of the initial condensate  $r_c = 4 \mu\text{m}$ . For example, for a BEC of  ${}^7\text{Li}$  atoms in the state (2,2) with negative scattering length  $a = 1.4 \times 10^{-7} \text{ cm}$ , the atom number in the initial condensate is  $N = 1.4 \times 10^4$  with a BEC length  $L_c = 60 \mu\text{m}$  and a radius of  $r_c = 4 \mu\text{m}$ . In the case of lithium atoms, the time scale  $t_c = 1 \text{ ms}$ . The wave length of optical radiation which forms the optical lattice can be chosen as  $\lambda = 40 \mu\text{m}$  [13] which leads to  $kz_c = 0.3$ , i.e. inequality (12) is satisfied.

We have to point out that there are periodical oscillations of the width and amplitude of these solitons as a result of the interaction between the BEC and the optical lattice (see Fig. 2b). They cannot be considered as internal modes of one-dimensional BEC solitons because, firstly, they disappear together with the switching off of the optical field and, secondly, the appearance of internal modes requires sufficiently strong non-locality of interatomic interaction in a BEC [14]. Therefore we can identify such structures after switching off the optical lattice as ordinary spatial solitons. The wavefunctions of these solitons can be assumed to take the form

$$\Phi_s^\pm = \frac{\sqrt{B/2}}{\cosh[B(z \mp vt)]} \exp(i\gamma t \pm ik_s z), \quad (14)$$

where  $B = 2\pi a N_s / \sigma$ ,  $\gamma = (B^2 - k_s^2)\hbar/2M$ ,  $v = \hbar k_s / M$ . The functions  $\Phi_s^\pm$  are well-known exact solutions of equation (2) for the depth of optical potential  $V(z) = 0$ . Comparing soliton solutions from (2) and (4), we obtain the correspondence between atom number in a soliton,  $N_s$ , and the maximum value of the soliton wave function  $|\Psi_m|$  as

$$B = \frac{2\pi a N_s}{\sigma} = \frac{|\Psi_m|}{\sqrt{2} z_c}. \quad (15)$$

In the case shown in Figure 2b, the maximum value of soliton wave function  $|\Psi_m| = 1.8$  corresponds to a concentration  $N_{cs}^m = 2.3 \times 10^{13} \text{ cm}^{-3}$ . At the same time, the number of atoms in solitons equals  $2N_s = 7.2 \times 10^3$  and they contain  $\sim 51\%$  of the atoms of the initial BEC. As a result of interaction between the BEC and the optical lattice (see Fig. 2b), we have obtained two main coherent solitons moving in opposite directions from the point  $z = 0$  with small velocity  $v \approx 0.1 \text{ cm/s}$ , whereas the central soliton can be removed by switching off the local magnetic field.

We have to point out that the width  $w$  of the initial condensate along the  $z$ -axis, see equation (5), has been chosen in such a way that just the two main solitons of the condensate are generated [15]. To estimate the intensity of far-detuned optical radiation necessary to reach dimensionless potential depth  $V_0^c = (2Mz_c^2/\hbar^2)V_0 \approx 0.02$ , we consider the practical case of  ${}^7\text{Li}$  atoms with mass  $M = 1.2 \times 10^{-23} \text{ g}$ , a scattering length modulus of  $a = 27.6a_0 = 1.46 \times 10^{-7} \text{ cm}$ , and a dipole moment value of  $d = 6 \times 10^{-17} \text{ CGSE}$ . In this case the required intensity of the far-detuned laser can be estimated as  $P \approx 50 \text{ W/cm}^2$  with an optical detuning  $\Delta \approx 2.8 \times 10^{15} \text{ rad s}^{-1}$ . Such an intensity can be reached through focusing the radiation of a commercial available laser SIFIR (see website coheren-inc.com).

## 4 Precision measurements with a soliton interferometer

### 4.1 Interference of the BEC soliton states

To observe the interference of the two solitons generated by the interaction of the initial BEC with the optical

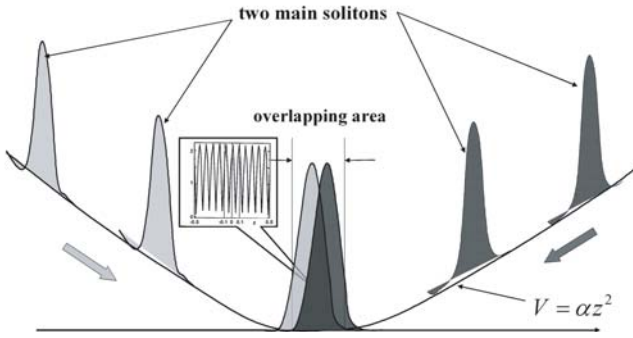


**Fig. 3.** Acceleration of solitons by the parabolic external magnetic field for different propagation times. The interference pattern is generated by the overlapping of two solitons (see the inset to the figure). The inset shows the spatial distribution of the wave function modulus  $|\Psi(z, t)|$  at the moment of complete overlap near the central position.

lattice, let us switch on the external parabolic magnetic field

$$V_{ex} = \alpha z'^2. \quad (16)$$

This field changes the direction of propagation of the solitons (see Fig. 3). Then, after their collision, the interference of the two solitons occurs. As the solitons are accelerated by the magnetic field (16), the corresponding distortions of soliton shape result in certain distortions of the interference pattern. The origin of this distortion is that different parts of the solitons have different values of acceleration due to the magnetic field (16). Therefore the quantity  $\alpha$  which determines the curvature of potential (16) is limited to a value of  $\alpha \leq 0.3$  (Fig. 3) which corresponds to  $\alpha \leq 10^{-17}$  erg/cm<sup>2</sup>. For larger values of  $\alpha$  the soliton shape may be lost, leading to the destruction of the interference pattern.

The inset in Figure 3 shows the spatial distribution of the wave function modulus  $|\Psi(z)|$  at the moment of complete overlap of the two solitons in the central region. According to equation (14), this distribution can be given in the form

$$|\Psi(z)| \sim |\Phi^+ + \Phi^-| \sim |\cos(k_s z)|. \quad (17)$$

The interference fringe width  $\Delta z$  is determined by the final velocity  $v_{final}$  of the solitons:  $\Delta z = \pi/k_s = \pi\hbar/(Mv_{final})$ .

It should be remarked that the solitons passing through the magnetic waveguide lose atoms due to two-particle collisions causing the inversion of atomic spin. This leads to a change in the soliton shape. Assuming that the rate of this change is slow enough, we obtain the equation describing the time evolution of the atom number in soliton [9]

$$\frac{dN_s}{dt} = -\frac{\beta a N_s^3}{\sigma}, \quad (18)$$

where the rate of two-particle collisions  $\beta = 10^{-14}$  cm<sup>3</sup>/s [16]. The solution of equation (18) can be obtained in the form

$$\left( \frac{1}{N_s^2} - \frac{1}{N_{is}^2} \right) = \frac{2\beta a}{\sigma^2} t,$$

which describes the decrease in atom number compared to the initial value  $N_{is}$ .

The critical temperature which corresponds to the maximum concentration in the solitons after interaction with the optical lattice is twice higher than the temperature of the initial condensate. By propagation of the solitons, their concentration decreases, ending to a decrease of their critical temperature. As the result, a value of critical temperature  $T_{cr}$  for the soliton corresponding to that of the initial condensate is reached in a propagation time of  $t \approx 10$  s. At the same time, the soliton width increases from  $2 \mu\text{m}$  up to  $6 \mu\text{m}$ , and the number of atom in solitons is decreases up to  $N_s = 2 \times 10^3$  in each soliton.

#### 4.2 Sensitivity of interference pattern to magnetic field gradient

Let us consider now the possibility of the precise measurement of a magnetic field gradient based on the observation of the interference pattern of the BEC solitons. As one can see from Figure 2, after interaction of the BEC with the optical lattice, two coherent solitons appear moving in opposite directions from the point  $z = 0$  with small velocity  $v \approx 0.1$  cm/s. For an observation time  $t_0 \approx 10$  s the distance between the two main solitons is approximately equal to  $2z_0 \approx 2$  cm.

Let us assume that a weak inhomogeneous magnetic field  $H(z)$  is applied, and that this field influences the solitons during their propagation. As a result, these solitons acquire an acceleration  $a = -(\mu_0/M)\partial H_z/\partial z$  with the Bohr magneton  $\mu_0 = 0.9 \times 10^{-20}$  erg/Gs and therefore both solitons will be shifted relative to the points  $\pm z_0$  by a distance

$$\delta = \frac{at_0^2}{2} = 4 \times 10^4 \frac{\partial H}{\partial z}. \quad (19)$$

Therefore, switching on an external parabolic magnetic field  $V(z) = \alpha z^2$  with a curvature  $\alpha = 1.6 \times 10^{-22}$  erg/cm<sup>2</sup>, we change the initial propagation directions of these solitons. As a result the solitons will arrive at the point  $z = 0$  with velocities  $v \approx 5$  cm/s. The flight time of solitons in a parabolic potential does not depend on the initial soliton position. At the same time the localization of the interference pattern near the point  $z = 0$  depends on the phase shifts of the colliding BEC solitons which are given by the following expressions:

$$\varphi_+ = \frac{M}{\hbar} \int_{-(z_0+\delta)}^z v_+ dz, \quad \varphi_- = \frac{M}{\hbar} \int_z^{z_0-\delta} v_- dz, \quad (20)$$

$$v_{\pm} = \left\{ \frac{2\alpha}{M} [(z_0 \pm \delta)^2 - z^2] \right\}^{1/2}.$$

Here the quantity  $\varphi_+$  (or  $\varphi_-$ ) determines the phase shift of soliton moving in the positive (or negative) direction of the  $z$ -axis. Substituting equation (16) into equation (14)

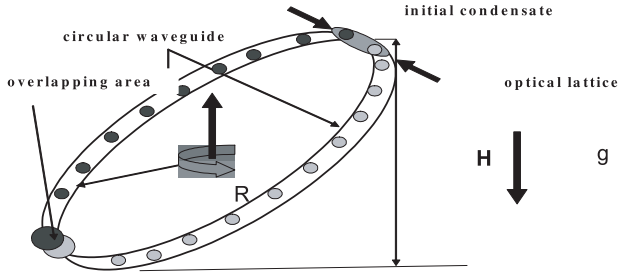


**Fig. 4.** The soliton-two-input interferometer as a gyroscope. Initially, the formation of the spatial solitons in the BEC with negative scattering length by the optical lattice (1) occurs. After that each of the two solitons is loaded into the magnetic waveguide ring (one of the solitons shown as black circle is loaded to the left hand side of magnetic ring and the other soliton – the gray circle – is loaded to the right hand side). These solitons are accelerated by gravity and collide at the lowest point of the waveguide ring. The interference pattern is formed in the overlapping soliton area.

we can obtain the spatial dependence of the wave function modulus  $|\Psi(z)|$  for the time of complete overlap between the two solitons at the point  $z = 0$  in the form

$$|\Psi(z)|^2 \sim |e^{i\varphi_+} + e^{i\varphi_-}|^2 \approx \cos^2(k_s[z + \pi\delta/2]). \quad (21)$$

As one can see from equation (17), the position of the fringes depends on the displacement  $\delta$  which is proportional to the gradient of the magnetic field, equation (15). Assuming that the displacement  $\delta = \delta_f = \pi/2k_s$ , we can estimate the precision of the measurement of magnetic field gradient as

$$\frac{\partial H}{\partial z} = 10^{-9} \text{ Gs/cm} = 10^{-2} \text{ pT/cm}. \quad (22)$$

At the same time, the wave number of the interference pattern is about  $k_s = 6 \times 10^4 \text{ cm}^{-1}$ ; this value of  $k_s$  has been obtain with a soliton velocity  $v_{final} \approx 5 \text{ cm/s}$ . At the same time, each interference fringe contains approximately 200 atoms.

### 4.3 Measurement of angular rotation

In the previous section we have considered the possibility of performing precision measurements of a magnetic field gradient with an atom wave interferometer which uses in its arms BEC solitons instead of single atoms. Let us now consider how this type of interferometer can be applied to the measurement of an angular rotation. For this purpose we use solitons inside a Sagnac interferometer. To realize this type of interferometer, these solitons which are initially generated by an optical lattice should be put into a magnetic waveguide ring with radius  $R$  (Fig. 4). The plane of this ring is inclined to the horizontal plane at an angle of about  $H/2R$  where  $H$  is the inclination height. Each soliton is accelerated by gravity, and they collide at the lower point of the ring (Fig. 4). In this area, an interference pattern with the period  $1/k_s$  is formed. The wave

number of the pattern  $k_s$  is determined by the velocity that the solitons acquire in the waveguide

$$v_f = \sqrt{2gH}, \quad (23)$$

where  $g$  is the gravitational acceleration.

To obtain an interference pattern wave number as above, the value of  $H$  must be  $H \simeq 0.015 \text{ cm}$ . In this case, the propagation time  $\tau_s$  of the solitons in the ring can be obtained as

$$\tau_s = \int_0^{\pi r} \frac{dl}{v} = \frac{2R}{v_s} K(r), \quad r = \sqrt{2/(2+\gamma)}, \quad \gamma = 2(\nu_i/\nu_s)^2 \quad (24)$$

where  $K$  is the elliptic integral of the first kind, and  $\nu_{i,s}$  are the initial and final velocities of the solitons. For the maximum propagation time  $\tau_s \simeq 10 \text{ s}$ , the initial and final velocities are  $v_i = 0.1 \text{ cm/s}$ , and  $v_f = 5 \text{ cm/s}$ , which correspond to  $K = 5.4$ , and the radius of the ring which determines the precision of the rotation measurements is given by  $R \leq 4.6 \text{ cm}$ . To increase the precision measurement of angular rotation we accelerate solitons when they begin to move along the ring by switching on an external magnetic field with the potential (16) where  $\alpha = 6 \times 10^{-22} \text{ erg/cm}^2$ . As a result, the soliton velocity increases much faster as compared to the case when the external field is absent; e.g., the soliton velocity is  $2 \text{ cm/s}$  after an interaction time of  $0.4 \text{ s}$  with the potential (16). The time during which the external magnetic field acts on our system is much less than the propagation time  $\tau_s \approx 10 \text{ s}$ . Therefore assuming this as the initial soliton velocity we can estimate the radius of the ring to be  $R \simeq 10 \text{ cm}$ .

Let us assume that our setup rotates with an angular velocity  $\Delta\omega$ . Then, the interference pattern will shift relative to the lower point of the ring on the value  $\Delta\omega R\tau_s$ . In this case the precision of an angular rotation measurement  $\Delta\omega_{\min}$  can be determined to be the change of angular velocity, which leads to an interference pattern shift of  $\pi/2k_s$ :

$$\Delta\omega_{\min} = \frac{\pi}{2k_s R\tau_s} = 2.6 \times 10^{-7} \text{ rad/s} = 3.5 \times 10^{-3} \Omega_e, \quad (25)$$

where  $\Omega_e$  is the Earth's rotation velocity. We have to point out that the precision of such a method is much higher compared to the measurement of angular rotation based on a rotating interferometer with cooled atoms [17].

## 5 Summary

We have shown that the use of the soliton states of a Bose-Einstein condensate with negative scattering length in an atom interferometer allows us to make precision measurements of both magnetic field gradient and angular velocity. We have demonstrated that the sensitivity of such a soliton interferometer to variations of magnetic field can reach  $10^{-9} \text{ Gs/cm}$ . This value of sensitivity is much better compared to known methods. We have to point out that the sensitivity of soliton Sagnac interferometer is ten

times higher than the ultimate sensitivity of a gyroscope based on cooled atoms [4]. At the same time, we do not discuss here the ultimate sensitivity of the soliton interferometer because it is not limited by quantum noise (unlike an interferometer based on cooled atoms).

This work was supported by the Russian Foundation for Basic Research, grant #06-02-16562a, and by the Russian Ministry of Education and Science, grant RNP. 2.1.1.1189.

## References

1. M.G. Moore, P. Meystre, Phys. Rev. Lett. **83**, 5202 (1999); P. Meystre, *Atom Optics* (Springer-Verlag, New York, 2001)
2. Y. Castin, "Bose-Einstein condensation in atomic gases: simple theoretical results", [arXiv:cond-mat/0105058](https://arxiv.org/abs/cond-mat/0105058)
3. B.P. Anderson, M.A. Kasevich, Science **282**, 1686 (1998)
4. J.P. Dowling, Phys. Rev. A **57**, 4736 (1998)
5. K.E. Strecker, G.B. Partridge, A.G. Truscott, R.G. Hulet, Nature **417**, 150 (2002)
6. L. Khaykovich, F. Shreck, G. Ferrari, T. Bourdel, J. Cubizolles, L.D. Carr, Y. Castin, C. Salomon, Science **296**, 1290 (2002)
7. W. Ketterle, Phys. Today **52**, 30 (1999)
8. N.N. Rosanov, V.A. Smirnov, Yu. V. Rozhdestvensky, S.V. Fedorov, JETP Lett. **77**, 84 (2003)
9. Yu. V. Rozhdestvensky, N.N. Rosanov, V.A. Smirnov, JETP Lett. **76**, 370 (2002)
10. R.Y. Chiao, E. Garmire, C.H. Townes, Phys. Rev. Lett. **13**, 479 (1964)
11. V.I. Bespalov, V.I. Talanov, Sov. Phys. JETP Lett. **3**, 307 (1966)
12. V. Bagnato, D.E. Pritchard, D. Kleppner, Phys. Rev. A **35**, 4354 (1987)
13. A.A. Vedenov, G.D. Mylnikov, D.N. Sobolenko, Physics Uspekhi **138**, 477 (1982)
14. P.I. Krepostnov, V.O. Popov, N.N. Rosanov, JEPT **99**, 279 (2004)
15. N.N. Rosanov, V.A. Smirnov, Yu. V. Rozhdestvensky, S.V. Fedorov, N.A. Veretenov, D.V. Skryabin, W.J. Firth, Proc. SPIE **5402**, 98 (2004)
16. A.J. Moerdijk, B.J. Verhaar, Phys. Rev. A **53**, R19 (1996)
17. A. Lenef, T.D. Hammond, E.T. Smith, M.S. Chapman, R.A. Rubenstein, D.E. Pritchard, Phys. Rev. Lett. **78**, 760 (1997)